Acoustic Properties of Snow*

By

Tamotsu ISHIDA

石 田 完

Meteorological Section, The Institute of Low Temperature Science

Received January 1965

Abstract

The specific acoustic impedance of snow layers backed with rigid walls was measured by an acoustic tube method. The normal absorption coefficient of the snow layers was calculated, using the resistance and reactance values of the acoustic impedance. The frequency dependence of the normal absorption coefficients showed maxima in the frequency range in which the acoustic impedance was real. The sound velocity in the snow layers was calculated using this data. The sound transmission loss of white noise in snow layers was measured, and the attenuation constant in snow was calculated from the observed values of the transmission loss for samples of various thicknesses. Propagation of white noise on the surface of a snow cover and in a snow tunnel and trench was investigated. Parallel correlations between attenuation and absorption constants were observed in frequency-response curves obtained in the laboratory and in the field.

1. Introduction

Up to this time, there have been several studies of the acoustic properties of snow by Japanese investigators. ANDŌ and HOSOKAI (1952) studied the attenuation of sound in snow covers. FURUKAWA (1953) and ŌURA (1953 b) reported the absorption of sound in snow covers. ISHIDA and ONODERA (1954) examined the absorption coefficients of snow samples in the laboratory. TAKEDA, *et al.* (1954) measured the absorption coefficient of snow covers and studied the propagation of sound on their surfaces. The velocity of sound in snow was measured by ŌURA (1953 a). However, none of these studies have very well clarified the relation between the acoustic properties of snow and its

* Contribution No. 708 from the Institute of Low Temperature Science.

internal structure.

Many studies of sound absorbing meterials have revealed that the acoustic properties of these materials are highly dependent upon their internal structure. Snow is considered to be a kind of sound absorbing material which consists of fine, irregular ice-particles joined together. Since sound waves in snow may propagate by oscillation of air molecules in cavities or spaces in the snow, the acoustic properties may depend upon porosity, grain size and shape, and the three dimensional distribution of air spaces. The primary purpose of the present investigation was to provide knowledge of the fundamental acoustic properties of snow: acoustic impedance, attenuation and absorption coefficients, and transmission loss. The experiments were conducted in the laboratory and open snow fields using recently developed acoustic techniques. The observed sound propagation on the snow field was well explained by the acoustic properties of snow determined in the laboratory. One of the primary results of this study is the clarification of the relation between acoustic properties and the internal structure of snow by the thin section method and measurement of the flow resistance or air permeability of snow. Air permeability is also strongly dependent upon the structure of snow and is closely correlated to the acoustic properties. Measurement of the air permeability in snow was made by a flow meter developed by the author.

II. Method for Measuring Acoustic Impedance

Various methods and devices for measuring the acoustic impedance of porous materials have been developed by many investigators. The primary part of these devices consists of a cylindrical tube made of precision seamless steel tubing, with which to create plane travelling sound waves. A piece of the test sample and a sound source are placed at either end of this tube. When a sound wave is emitted from the source at one end of the tube, a steady sound field is produced within the tube by the interference of the travelling and reflective waves. This steady sound field may be sensitively modified by the acoustic impedance of the sample placed at the other end of the tube. Therefore, the acoustic impedance of a given sample is obtained by measuring the sound pressure distribution in the tube. In this experiment, two different methods were used to obtain the acoustic impedance of the samples. Several maxima or minima of the sound pressure were measured along the axis of a tube of constant length (constant length method), and the sound pressure of the acoustic resonance produced by varying the length of the tube was also measured at the source end of the tube (variable length method). In these experiments, the first method was used for small tubes (inside diameter: 3.15 cm, length:

90 cm) and high frequencies (up to 6,000 c/s), and the latter for large tubes (inside diameter: 8.9 cm, length: 99.9 cm) and low frequencies (up to 2,100 c/s).

The constant length method developed by WENTE and BEDELL (1928) and later modified by SCOTT (1946) has been the most common method of measuring acoustic impedance. A diagram of this technique is shown in Fig. 1. A specimen of snow is mounted in a detachable specimen holder, A, which

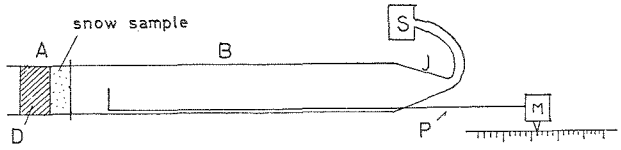

Fig. 1. Scott type impedance-measuring tube

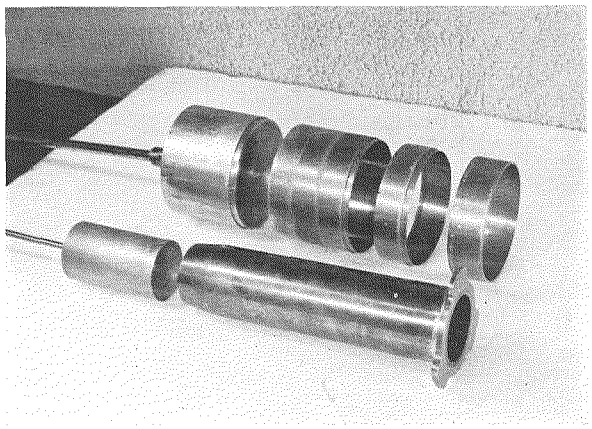

Fig. 2. Pistons and specimen holders

Upper ones are used for 8.9 cm diameter tubes (BERANEK's type). Specimen holders are removable thin, cylindrical bronze shells, 1 mm thick, and 2 cm wide. Snow samples are placed in the shells which are attached to a movable bronze piston, and then fitted into the main tube. Lower ones are used for 3.15 cm diameter tubes (SCOTT's type). The specimen holder and the main tube are the same. One end of the holder has a thin cutting edge and the holder is combined with a snow sampler. The other end has three projections which allow it to be attached to a flange on one end of the main tube

is closed at one end by a massive, close-fitting brass piston, D, (hatching). This is combined with a snow sampler as is shown in Fig. 2. The sound waves produced by the moving-coil loud-speaker unit, S, are emitted into the

main tube, B, through the conical end-piece, J. The steady sound field in the tube is explored with a moving probe-microphone, M, which consists essentially of the small diameter tube, P, which is moved along the length of the main tube. The position of the microphone can be accurately measured by a vernier-cursor sliding over a steel metre scale graduated in millimetres.

If α is the attenuation constant for a sound wave resulting from energy dissipation on the walls of the tube and in the inner air, and $k=\omega/c$, where ω is the angular frequency and c is the velocity of sound; $(\alpha/k)^2 \ll 1$ is generally satisfied. Then, the acoustic impedance*, Z, at the surface of the sample under test is given by

$$\frac{Z}{\rho_0 c_0} = \coth(\psi_1 + j\psi_2). \tag{1}$$

If a sound field of appropriate frequency is set up in the tube, and the probe microphone is moved along the length of the tube, successive maxima and minima of sound pressure may be observed at varying distances from the surface of the sample, as is shown in Fig. 3. Then, the ratio of the Mth maximum, $p_{\max}$, to the Nth minimum $p_{\min}$ is given by

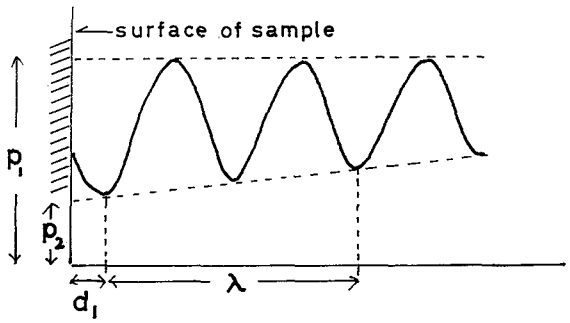

Fig. 3. Typical pressure-distance graph

$$\left|\frac{p_{\max}}{p_{\min}}\right| = \left[\frac{2\cosh^2(\alpha D_M+\psi_1) - \frac{\alpha^2}{2k^2}\sinh^2 2(\alpha D_M+\psi_1)}{2\sinh^2(\alpha d_N+\psi_1) + \frac{\alpha^2}{2k^2}\sinh^2 2(\alpha d_N+\psi_1)}\right]^{\frac{1}{2}}, \tag{2}$$

* This should be precisely described as the specific acoustic impedance of a sound medium on a given surface lying in a wave front, which is defined as the complex quotient of the sound pressure (force per unit area) on that surface, divided by the linear velocity (centimetres per second). The unit is dyne·s/cm³. The specific acoustic impedance is usually expressed by a dimensionless quantity (specific impedance ratio) which is the ratio of that impedance to the characteristic impedance of free space, $\rho_0 c_0$ (ρ_0: density of air, c_0: velocity of sound propagation in free space).

where D_M is the distance from the place at which the sound pressure is a maximum, to the surface of the sample, and d_N is the distance from the place at which the sound pressure is a minimum, to the surface of the sample. If we draw two tangential lines (dashsed lines) for the maxima and minima, as is shown in Fig. 3, the maximum and minimum values of the sound pressure p_1, p_2 on the surface of the sample may be obtained by extrapolation of these two lines. The maximum and minimum values p_1, p_2, are the quantities that would have been obtained if there were no dissipation in the tube, that is, if α had equaled zero. Puting $\alpha=0$ in Eq. (2), we can replace $|p_{\max}/p_{\min}|$ with $|p_1/p_2|$. Then, the real part ϕ_1 of Eq. (1) is given by

$$\phi_1 = \coth^{-1}\left|\frac{p_1}{p_2}\right|. \tag{3}$$

If d_1 is the distance from the surface of the sample where the first minimum occurs, the imaginary part ϕ_2 of Eq. (1) is expressed by

$$\phi_2 = k\left(\frac{\lambda}{4} - d_1 - \frac{\alpha}{2k^2}\sinh 2\phi_1\right), \tag{4}$$

where λ is the wave length measured from the interval between two minima.

The variable length method given by BERANEK (1940) is illustrated in Fig. 4. The test sample is mounted on a movable piston at one end of the

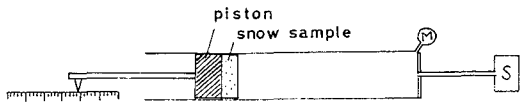

Fig. 4. Impedance-measuring tube (BERANEK's type)

tube as is shown in Fig. 4. The probe microphone, M, and a small tube, are attached to the edge of the same end of the tube where the sound source, S, is. The sound source is considered to be a point source of very high impedance, because the sound energy is emitted through a narrow barss tube filled with many straight copper wires.

The specific impedance ratio, $Z/\rho_0 c_0$, at the surface of the test sample is given by

$$\frac{Z}{\rho_0 c_0} = \frac{1}{1+j\dfrac{k_m}{\omega_m}} \cdot \coth\left[(k_m - j\omega_m)\frac{l}{c}\right], \tag{5}$$

where l is the length of the tube measured from the surface of the sample to the plane of the sound source and the microphone; k_m is the damping constant associated with absorption at the test sample; ω_m is the normal angular frequency of longitudinal vibration. When the length of the tube or the driving frequency is adjusted to give a maximum of sound pressure, the value of ω_m becomes

$$\omega_m = (\omega^2 - k_1^2)^{\frac{1}{2}} . \qquad (6)$$

If the driving frequency is held constant and the piston is moved along the axis of the tube, the probe microphone may detect an acoustic resonance at a certain length of tube. A typical resonance curve for sound pressure, p, *versus* distance, l, is shown in Fig. 5. If we obtain l' and l'' at the both

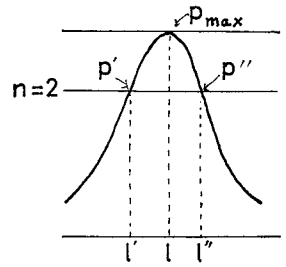

Fig. 5. Typical resonance curve

sides of the resonance curve where the square of the sound pressure, p, at the microphone is decreased to $1/n$ of its resonant value, the total daming constant, k_1, determined by the combined absorptions at the sample, the walls of the tube, the source, and the microphone is given by

$$k_1 \fallingdotseq \frac{\pi f(l''-l')}{l\sqrt{n-1}}, \qquad \left(\frac{p_{\max}}{p'}\right)^2 = \left(\frac{p_{\max}}{p''}\right)^2 = n . \qquad (7)$$

Then, when k_m/ω_m is small in comparison with 1, Eq. (5) becomes

$$\frac{Z}{\rho_0 c_0} = \coth\left[(k_1-k_0)\frac{l}{c} - j\frac{\omega}{c}\left\{\left(1-\frac{k_1^2}{2\omega^2}\right)l - l_0\right\}\right], \qquad (8)$$

where k_0 and l_0 are the damping constant and the resonant length of the tube with no sample; ω is the driving angular frequency; c is the velocity of sound in the tube. In Eq. (8) the following three approximations should be satisfied:

1) $k_m < 0.1\ \omega_m$

2) $l'^2 + l''^2 \fallingdotseq 2\,l^2$

3) $\lambda > 1.707\ D$

where λ is the wave length of the driving sound in the tube, and D is the inside diameter of the tube.

The first approximation is satisfied by choosing the length of the tube so that k_m may be sufficiently small, because k_m is inversely proportional to the length of the tube. In the present experiments the first approximation was always satisfied, since the resonant length of the tube was more than the wave length used.

The second approximation is almost satisfied, unless too broad a width, $(l''-l')$, is chosen for the resonant curve. In this experiment, the width of the curve of the sound pressure was measured at locations where the sound pressure was reduced to one half of that of the maximum; or $n=4$. The maximum deviation of k_1 from the average value was only ± 2 percent, even when k_1 was measured at any pressure ratio between $n=1.44$ and $n=6.76$.

The third approximation is the condition under which plane progressive waves may be set up in a tube. If the highest frequency at which measurements are to be made does not exceed the value given by 19,000/(the inside diameter of the tube in cm) at temperatures above -10°C, the third approximation is always satisfied.

When the specific impedance ratio is written by Eq. (1), the real and imaginary components of the acoustic impedance are calculated from

$$\left.\begin{aligned} \frac{R}{\rho_0 c_0} &= \frac{\sinh 2\phi_1}{\cosh 2\phi_1 - \cos 2\phi_2}, \\ \frac{X}{\rho_0 c_0} &= \frac{-\sin 2\phi_2}{\cosh 2\phi_1 - \cos 2\phi_2}. \end{aligned}\right\} \qquad (9)$$

R and X are, respectively, the acoustic resistance and the acoustic reactance. In this paper, all of the specific acoustic impedances of snow are expressed by acoustic resistance and reactance in $\rho_0 c_0$ units.

When a plane sound wave is emitted on the surface of a sample with a normal incident angle, the absorption coefficient, a, of the sample is given by

$$a = 1 - \left| \frac{Z-\rho_0 c_0}{Z+\rho_0 c_0} \right|^2. \qquad (10)$$

If we use values for R and X which are obtained by measuring the acoustic impedance of the sample, the absorption coefficient, a, can be expressed by

$$a = \frac{4R}{(R+1)^2+X^2} . \tag{11}$$

III. Method for Measuring the Flow Resistance

Propagation of a sound wave through a porous medium is strongly influenced by its porosity, shape and the distribution of pores or cavities, because sound waves are propagated through porous media primarily by oscillation of air molecules in the pore. In order to determine the acoustic property of a porous material, it is first necessary to know its air permeability or its air flow resistance.

The resistance of porous material to stational air flow is given by DARCY's law:

$$\frac{\Delta p}{L} = \sigma \cdot v . \tag{12}$$

where σ is the flow resistance per unit thickness of material measured (specific flow resistance), in g/s·cm^3; Δp is the pressure difference between the two faces

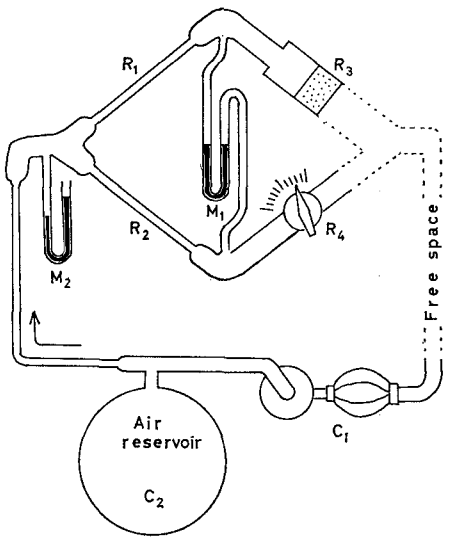

Fig. 6. Apparatus for measuring flow resistance

of a sample of thickness, L cm, in dynes/cm^2; v is the linear velocity of flow of air through the sample. Specific flow resistance may be used as a basic property of an acoustical material, because it corresponds to the real component of the specific acoustic impedance per unit thickness of the material when the sound frequency is zero.

In general, flow resistance has been measured according to DARCY's law, but a simple and compact apparatus for measuring the flow resistance of snow has been developed by ISHIDA and SHIMIZU (1956), the principle of which is analogous to a Wheatstone-bridge; that is, the flow resistance of snow is measured by comparison with an accurately calibrated variable standard of flow resistance. A diagram of the apparatus is shown in Fig. 6. The primary components of the Wheatstone-bridge, the constant resistance, variable resistance, galvanometer, and battery, were replaced by two narrow tubes, R_1, R_2, a variable leak-cock, R_4, an inclined-tube alcohol manometer, M_1, and a pressure source produced by a hand operating rubber-bellows, C_1. A cross-section of the variable leak-cook R_4, is shown in Fig. 7. A narrow cylindrical

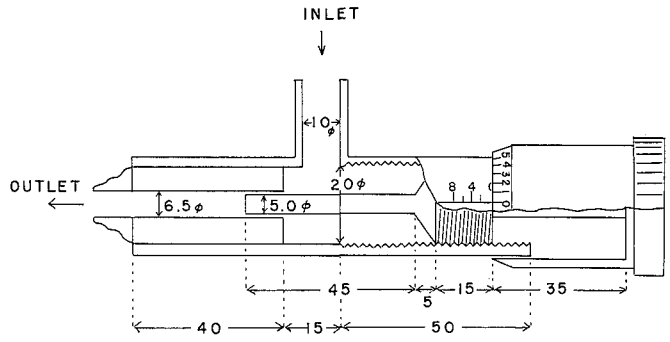

Fig. 7. Cross-section of leak-cock (dimensions in mm)

gap between a circular tube with an inside diameter of 6.5 mm, and a cylindrical rod 5.0 mm in diameter, is effective as a standard of flow resistance. The flow resistance of the leak-cock is varied by changing the length of the cylindrical rod inserted in the centre of the circular tube by turning screw, and the amount of flow resistance against the graduations on a dial in the screw is accurately calibrated. The snow sample is placed in the brass cylinder, R_3, (5 cm in diameter). The thickness of the sample should be previously adjusted so that its flow resistance may be brought within the limits of the measuring capacity of this bridge.

Typical operation of the apparatus is as follows: The rubber bellows, C_1,

is squeezed by hand and appropriate pressure is applied to the sample. The variable leak-cock, R_4, is adjusted so that the air flow through it is precisely equal to the flow through the snow sample. When these two air flows are equal, the alcohol manometer, M_1, indicates the same level. The flow resistance of the snow is obtained by reading a dial on the leak-cock.

In Fig. 8 the flow resistance measured by this method in various kinds of

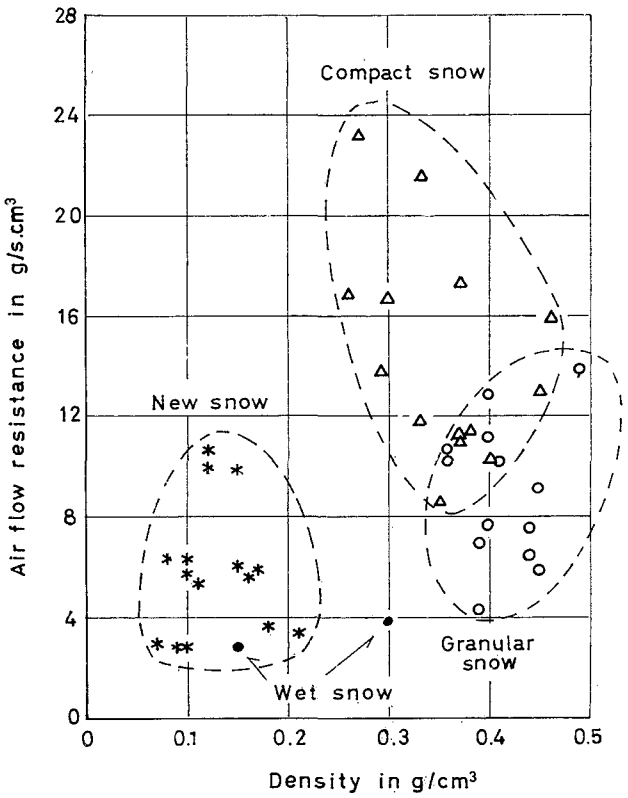

Fig. 8. Flow resistance of snow

snow are plotted against density. As is shown in this figure, in natural snow, the values for flow resistance are roughly grouped in three broad domains. This implies that the numerical value for the flow resistance of snow is not only determined by the density, but is also strongly dependent upon the internal structure. This is quite natural, because the shape or texture of the pores differs with every sample, even if the density is the same. Therefore, the acoustic impedance or air flow resistance of snow may be useful as an expression of its structure.

IV. Specific Acoustic Impedance of Snow Samples

The specific acoustic impedance of many kinds of snow samples with rigid wall backings were measured by both BERANEK's and SCOTT's method. All of the experiments were made at temperatures between 0 and −15°C. There are two modes of propagation of sound waves through a narrow tube. When a low frequency sound wave propagates through a fairly large tube, no temperature change is observed throughout the air in the tube, because the propagation may conducted under isothermal conditions. Therefore, the resistance of air flow in the tube may be given by POISEUILLE's law. However, when a high frequency sound wave propagates through a comparatively small tube, the air in the tube may vibrate adiabatically and cause appreciable temperature change. In this case, the resistance of the air flow may obey HELMHOLTZ's law. ZWIKKER and KOSTEN (1949) introduced a dimensionless number, μ, in order to establish a criterion for determining which type of sound propagation, isothermal or adiabatic, is taking place in porous materials. The dimensionless number μ is given by

$$\mu = \sqrt{8\omega k\rho_0/h\cdot\sigma}\ , \tag{13}$$

where ω is the angular frequency of sound; ρ_0 is the density of air; h is the porosity of a porous material; σ is its flow resistance, and k is the structure factor given by the square of the ratio of the sound velocity in free space to the sound velocity in the material. This value, μ^2, may be compared to REYNORDS' numbers in hydrodynamics. In acoustical engineering, propagation of sound is considered to be an isothermal POISEUILLE type when $\mu<1$, and an adiabatic HELMHOLTZ type when $\mu>10$.

If we use the following numerical values to calculate μ of snow:

$$\omega = 2\pi\cdot 400—2\pi\cdot 4{,}000$$
$$h = 0.6—0.9 \quad (\text{density}: \quad 0.37—0.09\ \text{g/cm}^3)$$
$$\sigma = 2—25\ \text{g/s}\cdot\text{cm}^3$$
$$k = 2—3$$
$$\rho_0 = 1.3\times 10^{-3}\ \text{g/cm}^3\ ,$$

we have

$$2<\mu<16\ .$$

Therefore, the sound propagation mechanism in snow is an intermediate case which is just between the two limits of isothermal and adiabatic. In this intermediate region, some fraction of the sound energy is dissipated in the air spaces which are surrounded by ice-particles, because of the phase difference between pressure and density changes in the air. Therefore, it is very difficult to express the acoustic impedance of snow in terms of material constants such as density, porosity, flow resistance, structure factor, and so forth. However, it is possible to express the acoustic impedance of new snow by analogy with an electric circuit, since its frequency dependence seems to be relatively simple.

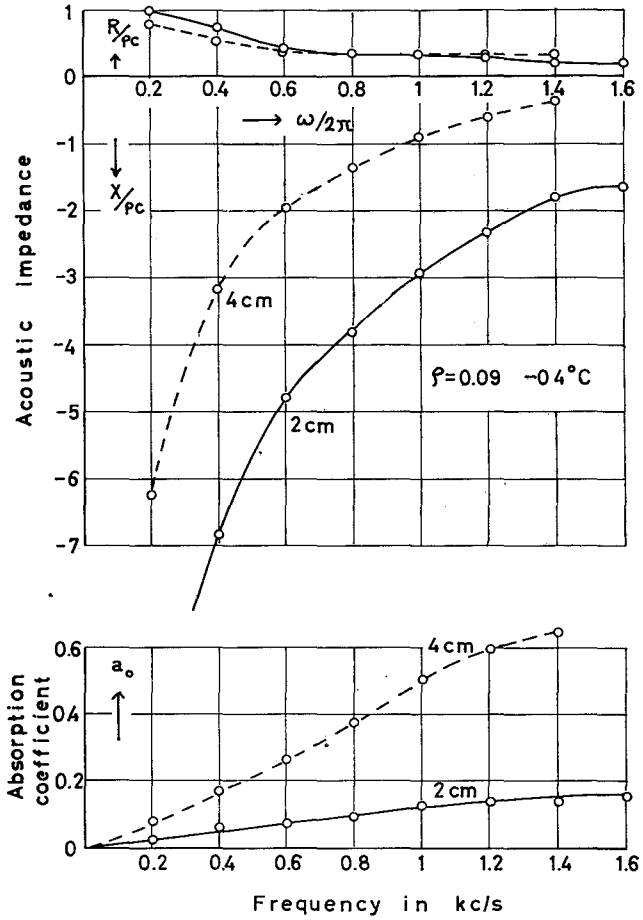

Fig. 9. Specific impedance of new snow
(density: 0.09 g/cm³, thickness: 2 and 4 cm)

1. *Impedance of new snow*

In Fig. 9, the frequency dependence of the real and imaginary components of the specific acoustic impedance of now snow (density: 0.09 g/cm³, thickness: 2 and 4 cm) is plotted in $\rho_0 c_0$ units; that is, as a ratio of the characteristic impedance of free space. The two lower graphs in this figure show the frequency dependence of the absorption coefficient of the same sample calculated from Eq. (11). The value for the real component of the impedance (acoustic resistance) is small and varies little against the frequency of sound, whereas the imaginary component of the impedance (acoustic reactance) has large negative values at low frequencies and its absolute values decrease parabolically

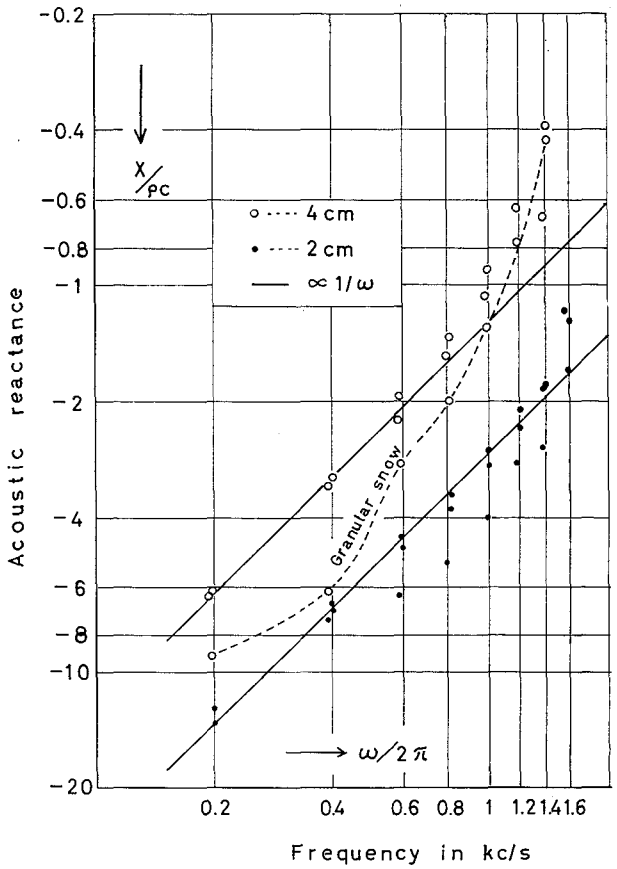

Fig 10. Acoustic reactance of new snow (density: 0.09, 0.10, and 0.13 g/cm³, thickness; 2 and 4 cm) and granular snow (density: 0.35 g/cm³, thickness: 4 cm)

with the frequency. This frequency dependence of the acoustic reactance is more clearly illustrated in Fig. 10. In this figure, the acoustic reactance of three samples of new snow (density : 0.09, 0.10, and 0.13 g/cm^3, thickness : 2 and 4 cm) and granular snow (density : 0.35 g/cm^3, thickness : 4 cm) is plotted against the frequency on log-log paper. The measured values for the acoustic reactance of new snow are distributed around two straight lines which slope at an angle of 45° to the abscissa, but the observed values for the acoustic reactance of granular snow deviate from a straight line. This means that the acoustic reactance of new snow must be only the acoustic capacitance. In addition, the acoustic resistance of new snow is nearly constant against frequency as is shown in Fig. 9. Therefore, the acoustic property of new snow may be explained by an acoustic model consiting of narrow tubes and large cavities, or by an electric circuit composed of electric series resistance, r, and shunt capacitance, C, as is shown in Fig. 11 a and b. The narrow tube and the large cavity in the acoustic model correspond to the resistance and capacitance in the electric circuit.

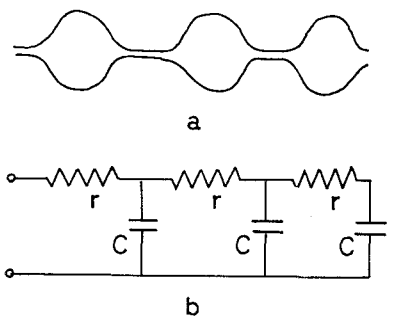

Fig. 11. (a) Acoustic model of new snow
(b) Electric circuit equivalent to (a)

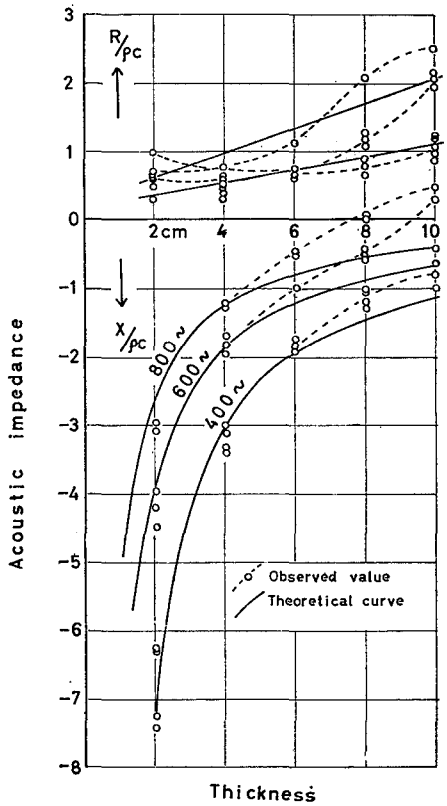

Fig. 12. Observed values of acoustic impedance of new snow and input impedance of its equivalent circuit

If we accept the validity of these two models for new snow, the following inference may be drawn : when a thin sample of new snow is represented acoustically by the above model, a thicker sample must be represented by a series of these models in proportion to its thickness. In order to prove this, the specific acoustic impedance of new snow

samples was measured as a function of the thickness of the samples. Figure 12 shows a comparison of observed and calculated values. The calculation was made by means of an electrical model in which T-sections (series resistance, r, and shunt capacitance, C) were increased one by one in proportion to thickness of the sample. The specific acoustic impedance corresponds to the input impedance of the electric circuit terminated at its far end by an infinite impedance. If n is the number of T-sections, resistance, R, and reactance, X, of the input impedance of the C-r recurrent network composed of n T-sections are given by

$$\left.\begin{aligned} R &= \frac{n^2+N+\left(\frac{N\cdot\omega rC}{n-1}\right)^2}{n^2+\left(\frac{N\cdot\omega rC}{n-1}\right)^2}\cdot r, \quad X = -\frac{n+\left(\frac{N\cdot\omega rC}{n-1}\right)^2}{n^2+\left(\frac{N\cdot\omega rC}{n-1}\right)^2}\cdot\frac{1}{\omega C}, \\ N &= \sum_{i=1}^{n-1}(n-i)^2 . \end{aligned}\right\} \quad (14)$$

For new snow, the acoustic resistance is very small compared with the absolute values for the acoustic reactance, unless the frequency is too high. Therefore, an approximation $r \ll 1/\omega C$ can be made in Eq. (14). Then, Eq. (14) becomes approximately

$$R \fallingdotseq \left\{1+\sum_{i=1}^{n-1}\left(1-\frac{i}{n}\right)^2\right\} r, \quad X \fallingdotseq -\frac{1}{n\omega C} . \quad (15)$$

The calculated values in Fig. 12 were obtained from Eq. (15) for reactanc at frequencies of 400, 600, and 800 c/s, and for the resistance for two appropriate values of r. The observed values of acoustic impedance *vs.* thickness for new snow samples (density: 0.1—0.2 g/cm^3) agree fairly well with the calculated curves. However, the observed values for reactance deviate from the calculated curves at high frequencies and larger thicknesses. These deviations may be produced in part by the approximation, $r \ll 1/\omega C$, but more by the fluid motion of the air mass in the narrow tube. That is, for a more complete model, series inductance should be added to the equivalent circuit.

2. *Impedance of compact snow*

The acoustic impedance of compact snow generally has smaller reactance and higher resistance than that of new snow, since its grain size and air spaces are fine and small because of natural compaction or densification. The ice grains in compact snow are usually rounded by metamorphism over long periods of

time. Figure 13 shows thin sections with two grain structures typical of naturally compacted snow. The thin section was made by the anilin method developed by KINOSITA and WAKAHAMA (1959). Though these two samples have almost the same density (0.31 and 0.32 g/cm^3), the size and shape of the

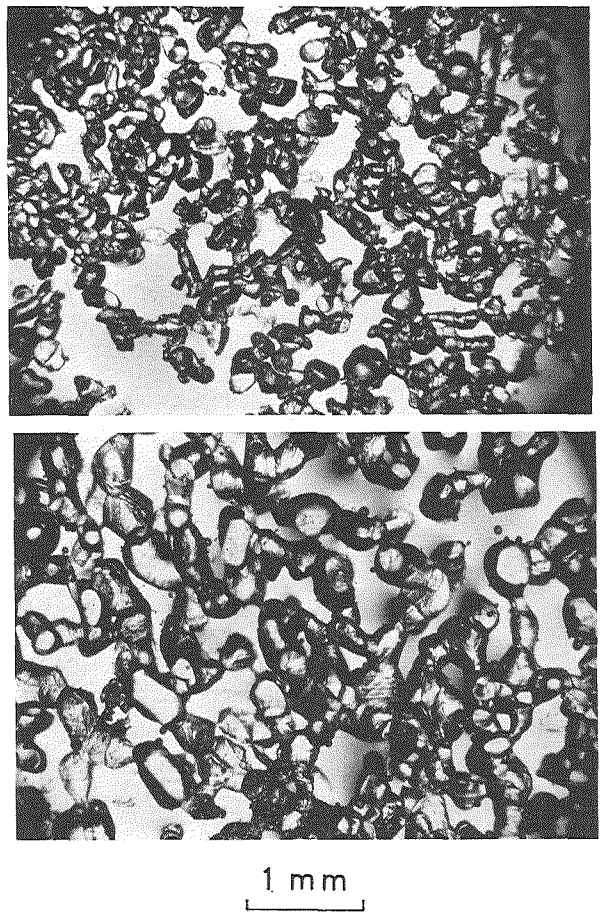

Fig. 13. Thin sections of two samples of compact snow of almost the same density and different texture

grains are quite different. Sample D is relatively young snow and its grains are small and a little angulated, whereas sample E is old snow with large round grains. The frequency dependence of the reactance and resistance of these samples is shown in Fig. 14. The values for reactance are nearly the same in these two samples, but some difference may be seen in the values for

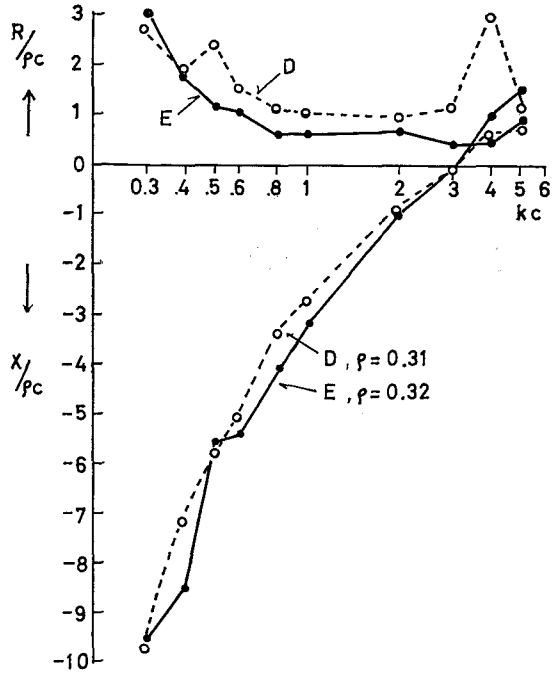

Fig. 14. Acoustic impedance of compact snow shown in Fig. 13

resistance. In all frequency ranges between 0.4 and 0.5 kc, the values for resistance were higher in sample D (young snow). The acoustic reactance of snow is primarily dependent upon the average volume of air spaces in it, therefore, the values for reactance are nearly equal for these samples which have nearly the same density. The acoustic resistance of snow is primarily dependent upon the size and tortuosity of the narrow tubes between ice particles. It is possible that the tubes surrounding the angular particles in sample D are narrower and more tortuous than those surrounding the round particles in sample E, and that the acoustic resistance of sample D may therefore be higher than that of sample E.

Figure 15 shows micro-photographs of thin sections from three samples of compact snow. In these figures, A is naturally compacted snow, density $\rho = 0.20$ g/cm^3 and B and C show the changes in internal structure in the same snow produced by artificial compression. Two blocks of snow 4 and 5 cm thick were gradually compressed to a thickness of 3 cm. The densities of the compressed snow samples were therefore increased from the original value

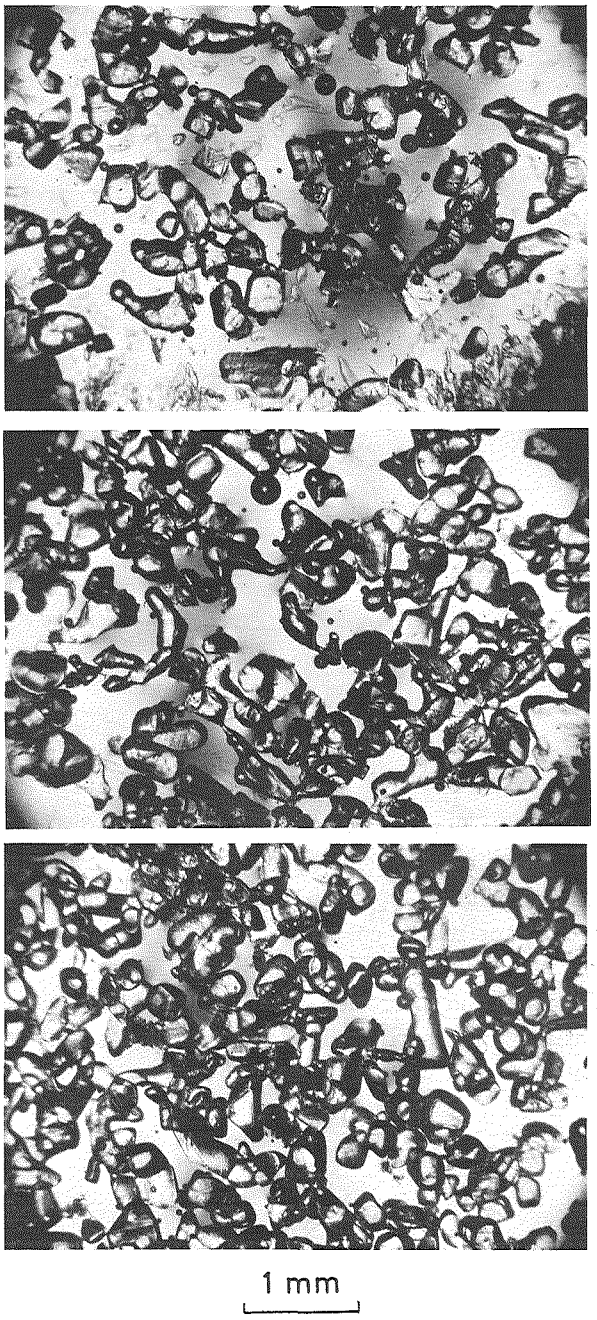

Fig. 15. Thin sections of compact snow

($\rho=0.20$) to $\rho=0.26$ (B) and $\rho=0.32$ g/cm^3 (C). Though there was no appreciable change in grain size or shape following compression, densification and compaction may be clearly seen in B and C in this figure. The change in the frequency dependence of the acoustic impedance in this compressed snow is shown in Fig. 16. As is shown in this figure, the values for resistance obviously increased with density in all frequency ranges between 0.5 and 4 kc, because

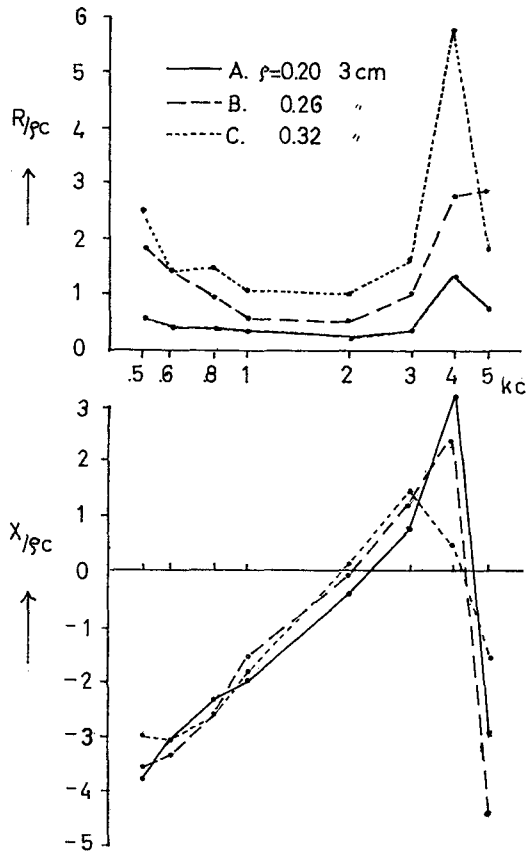

Fig. 16. Acoustic impedance of compact snow shown in Fig. 15

the more the snow is compressed, the more the tubes surrounding the ice particles are restricted. While, the increase of reactance resulting from compaction is insignificant, the maximum values for reactance, which appear around 4 kc, decrease with densification. This may be a result of the fact that the air mass which opposes a change in the volume current in the tube, is reduced

with densification. The reason why the values for reactance fall rapidly at 5 kc, may be that standing waves are formed by resonance within the samples as will be discussed later. These two experiments indicate that reactance in compact snow is not significantly influenced by the internal structure of the snow, in the density range between 0.2 and 0.3 g/cm^3, but resistance increases with density, and if the grain size or shape is different, the resistance varies, although the density remains the same.

3 .iii) *Suond velocity in snow*

When acoustic impedance is plotted in a complex plane, the contours along which the value of the absorption coefficient remains constant are circles in

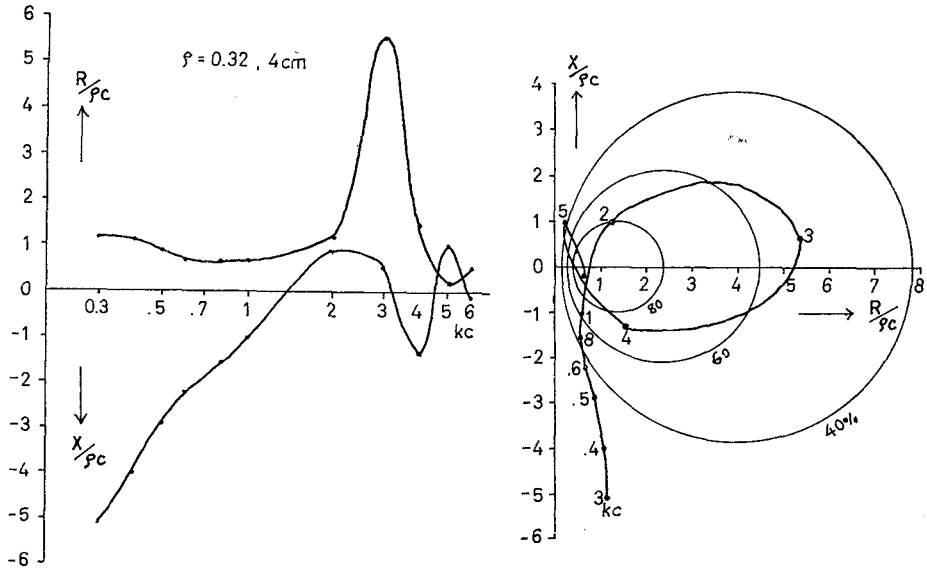

Fig. 17. Left, acoustic impedance *vs.* frequency for compact snow (density: 0.32 g/cm^3, thickness: 4 cm), and right, impedance contour

this plane. For 100% absorption the circle reduces to the point where the characteristic impedance of free space, $\rho_0 c_0$, is given. In Figs. 17 and 18, the acoustic impedance compact snow is plotted in the complex plane. As may be seen in these figures, impedance contours describe loops as the frequency or thickness of the sample increases. The absorption coefficient is maximum at the point where the impedance contour crosses the real axis in the neighbourhood of the characteristic impedance of free space. The absorption coefficients for the compact snow, obtained from Fig. 18, are plotted against thickness in

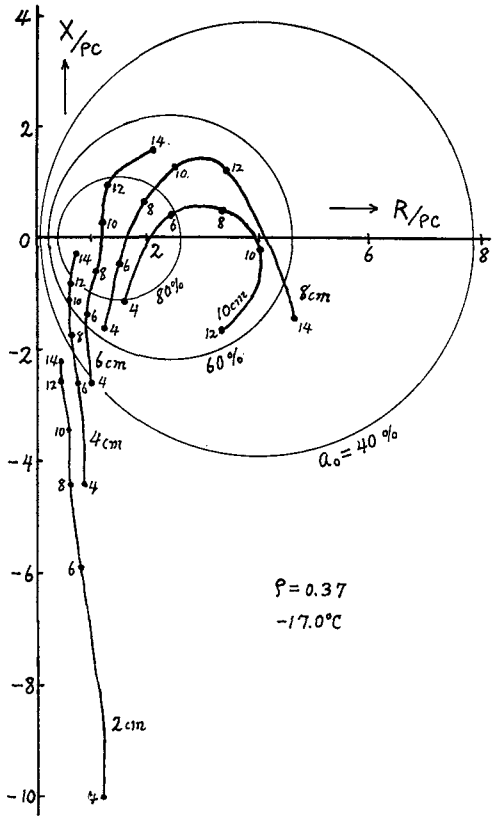

Fig. 18. Impedance contours of compact snow in 100 c/s

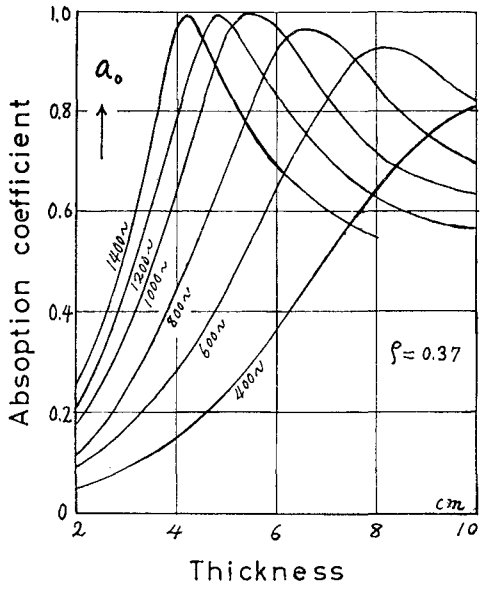

Fig. 19. Absorption coefficient of compact snow shown in Fig. 18

Fig. 19. When the absorption peak appears at a certain frequency in a sample of definite thickness, the standing wave may be maintained within the sample. In this case, a sample with a rigid wall backing may be acoustically regarded as a pipe, closed at one end and opened at the other. The fundamental resonant frequency of this equivalent pipe is given by

$$f=\frac{c}{4l}, \tag{16}$$

where l is the thickness of a sample and c is velocity of sound through the sample. Inserting the values for frequency and thickness at which maximum absorption is observed, into Eq. (16), we can calulate the velocity of sound through a sample as is shown in Fig. 20. It appears that the velocity of sound in compact snow of a definite density is proportional to the frequency, in the

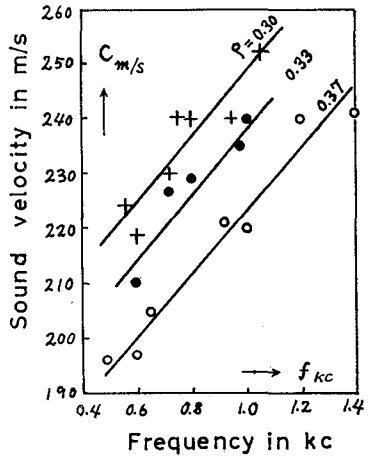

Fig. 20. Relation between the velocity and frequency of sound through compact snow layers

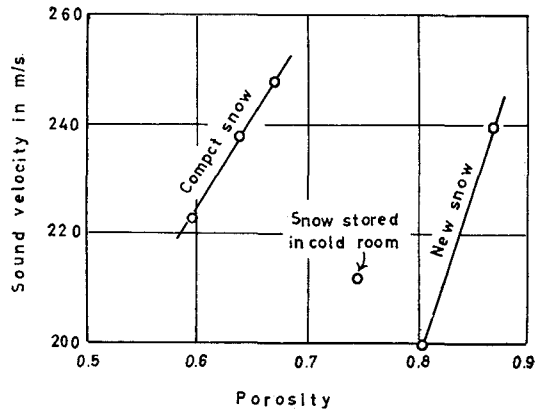

Fig. 21. Relation between the velocity of sound (1 kc/s) in snow and its porosity

range between 400—1,400 c/s. In Fig. 21, the porosity dependence of sound velocity measured at 1 kc is shown for three kinds of snow. A linear correlation between velocity and porosity is observed in compact and new snows in regions of quite different porosity. This implies that porosity is not the only determining factor in sound velocity in snow. However, in any kind of snow, the sound velocity can be expected to approach a definite value when the frequency approaches 0, and to the value for free space when the frequency approaches ∞.

We shall analyze the frequency dependence of sound velocity in snow using uniform transmission line in electrical engineering. When the distributed line-constants, resistance, inductance, conductance, and capacitance, are expressed by R, L, G, and C, respectively, the specific impedance, Z, and the admittance, Y, are given by

$$\left.\begin{aligned} Z &= R+j\omega L\,, \\ Y &= G+j\omega C\,. \end{aligned}\right\} \qquad (17)$$

Then, the input impedance, Z_s, for length l of this line terminated in infinite impedace is

$$Z_s = \sqrt{\frac{Z}{Y}}\coth\sqrt{Z\cdot Y}\,l\,, \qquad (18)$$

where $\sqrt{Z\cdot Y}=\alpha+j\beta$, α is the attenuation constant, $\beta(=\omega/c)$ is the phase constant, ω is the angular frequency, and c is the phase velocity. Multiplying

the first equation of (17) by the second equation of (17) and separating the real part from the imaginary part, we have

$$\left.\begin{aligned}\alpha^2 &= \frac{1}{2}\sqrt{(R^2+\omega^2L^2)(G^2+\omega^2C^2)}+\frac{1}{2}(RG-\omega^2LC)\,,\\ \beta^2 &= \frac{1}{2}\sqrt{(R^2+\omega^2L^2)(G^2+\omega^2C^2)}-\frac{1}{2}(RG-\omega^2LC)\,.\end{aligned}\right\} \tag{19}$$

Since $\beta=\omega/c$, the phase velocity is

$$c=\sqrt{2}\,c_0\left\{1-\frac{1}{x^2}+\sqrt{1+(4m^2-2)\frac{1}{x^2}+\frac{1}{x^4}}\right\}^{-\frac{1}{2}}, \tag{20}$$

where

$$m=\frac{1}{2}\left(\sqrt{\frac{RC}{GL}}+\sqrt{\frac{GL}{RC}}\right),$$

$$x=\omega\sqrt{\frac{LC}{RG}}\,,\qquad c_0=\frac{1}{\sqrt{LC}}\,,$$

and c_0 is the velocity of light for the line in a vacuum, and is the velocity of sound in free space for the propagation of sound.

Equation (20) becomes

$$c=c_0/m \qquad \text{for} \quad \omega=0\,,$$

and

$$c=c_0 \qquad \text{for} \quad \omega=\infty\,.$$

A curve of the velocity ratio c/c_0 in the case of $m=\sqrt{3}$ is shown as a function of x in Fig. 22. This curve indicates that the velocity of sound in snow

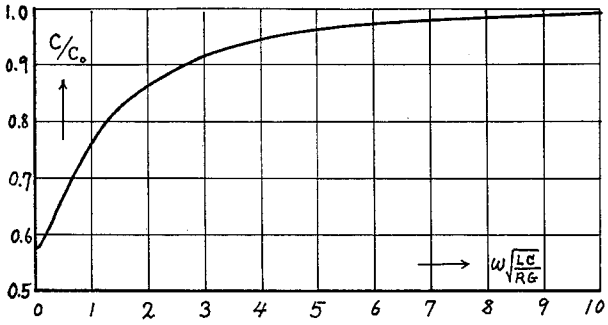

Fig. 22. Frequency characteristic of the phase velocity through a transmission line

increases with the angular frequency, ω, and asymptotically approaches the velocity of sound in free space for $\omega=\infty$.

V. Transmission Loss in Snow Samples

The general aspects of the absorption coefficients of snow layers have been described in the previous section. Attenuation of the energy of sound by the snow layers will be discussed in this section.

The transmission loss, TL, is defined by the decibel unit as follows:

$$TL = 10 \log_{10} \frac{\text{Intensity of incident sound}}{\text{Intensity of transmitted sound}} . \qquad (21)$$

In general, the TL of a material is measured by inserting a panel of the material in an opening between two reverberant rooms, the source and receiving rooms. In the present experiment, however, the following method was used: A trench, ($1 \times 11 \times 1.25$ m) was dug in an open snow field. The bottom of trench was almost at ground level. A tetragonal hole ($60 \times 40 \times 85$ cm) was made in the middle of the trench wall. A moving-coil loud-speaker mounted in an enclosed spherical cabient 40 cm in diameter, was placed in this hole as a sound source, and the mouth of the hole was sealed tightly with a snow-block 23 cm thick. As is shown in Fig. 23, the dimensions of the source room were therefore $62 \times 60 \times 40$ cm. After the snow-lid was examined and proved to be leak proof, an opening 15×15 cm was made in the centre of the lid to arrow emission of sound waves. A shallow step (5 cm wide and 5 cm deep) was constructed on the periphery of this opening to hold the snow samples. The snow cover in which this sound source room was made, was composed of uniform compact snow (density: 0.3–0.4 g/cm^3) lying more than 20 cm below the surface. A snow sample (25×25 cm) was placed in the opening. The thickness of the sample varied from 2 to 10 cm. The snow sample was always cut horizontally from deposited snow so that texture of the sample was as uniform as possible. Therefore, all of the values for transmission loss given in this paper are those

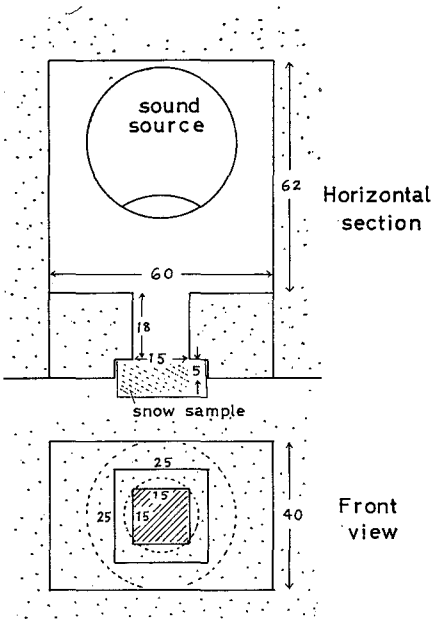

Fig. 23. Source room for measuring the transmission loss in snow layers (dimensions in cm)

obtained in cases where the sound was transmitted vertically through the snow cover.

White noise was produced by a generator and amplified and emitted from the lound-speaker. The frequency characteristics of the white noise are shown in Fig. 24. The intensity of the sound was measured in every 20 frequency band in the range from 100 to 8,000 c/s using a sound level meter and 1/3 octave band-pass filters. The frequency characteristics of the band-pass filters are shown in Fig. 25. The air temperature was $-7°C$ during the time the experiments were made.

If the method described above is used to measure the TL of snow, Eq. (21) can be substituted for

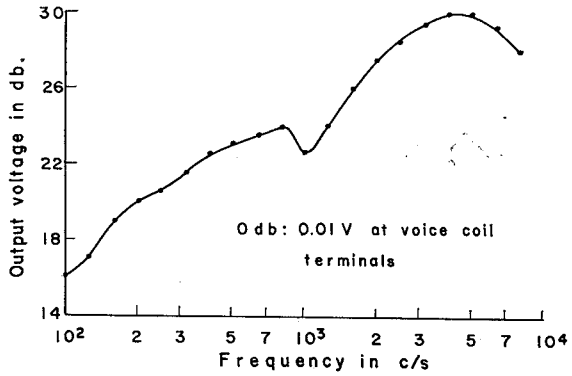

Fig. 24. Frequency characteristic of a white noise source in 1/3 octave bands

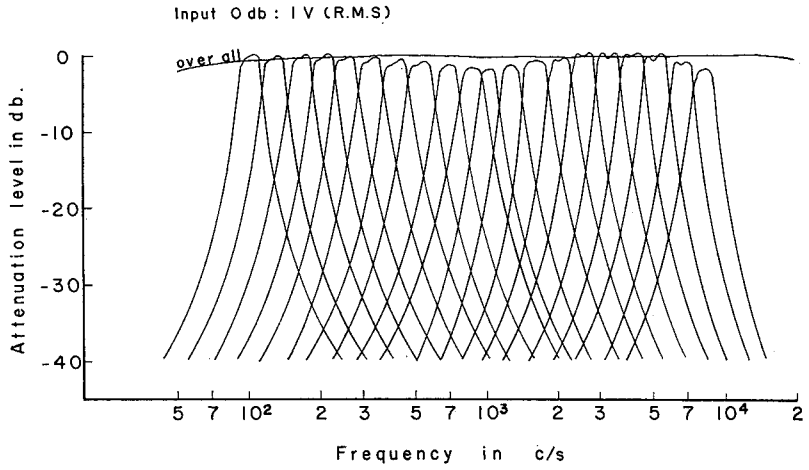

Fig. 25. 1/3 octave band-pass filter characteristics

$$TL = L_1 - L_2 , \tag{22}$$

where L_1 is the sound level at the face of the sample in the source room, and L_2 is the sound level at the other face of the sample in the receiving room. The trench-wall was located about 1 m beyond the receiving room, but L_2 was little influenced by reverberations from this wall.

Figure 26 shows the frequency dependence of the transmission loss in compact snow (density: 0.35 g/cm^3, flow resistance: 14.0 g/s·cm^3). The values of transmission loss for the overall band of white noise were 10.5 db for a thickness of 2 cm, 12.5 db for a thickness of 4 cm, and 15.5 db for a thickness

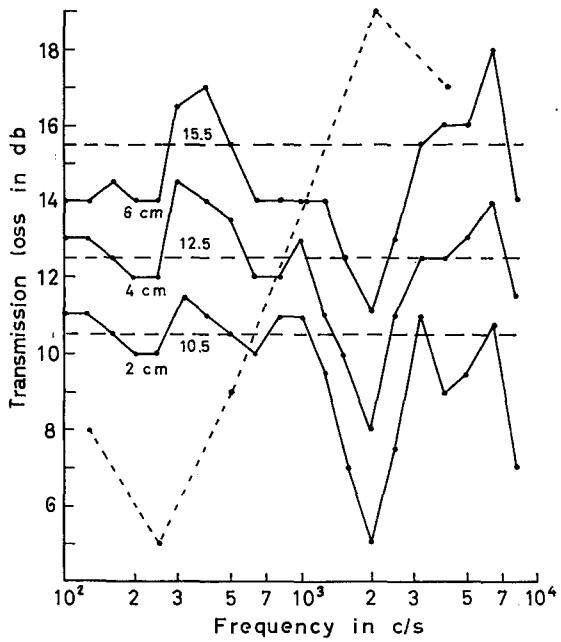

Fig. 26. Frequency characteristics of transmistion loss in compact snow (density: 0.35 g/cm^3, flow resistance: 14.0 g/s·cm^3). Broken line shows transmission loss through a hollow block of pumice-stone (surface density: 75.7 kg/m^2, thickness: 10.2 cm)

of 6 cm. In order to compare the frequency dependence of the TL in snow with that in other porous material, the transmission loss of a hollow block of pumice-stone, a kind of building-material, was plotted and is shown by the dotted line in Fig. 26. This sample had a surface density of 75.7 kg/m^2, and a thickness of 10.2 cm. It is generally known that the transmission loss of porous materials increases with frequency. The present experiment, however,

indicates that the frequency dependence of the TL in compact snow is quite irregular and has no tendency to increase with frequency.

In Fig. 27, the relation between the transmission loss and the thickness of the compact snow (density: 0.35 g/cm^3, flow resistance: 19.8 g/s·cm^3) is shown as a function of frequency. If the intensity of sound is decreased logarithmically against the distance of propagation through the snow layer, the sound pressure, p, at a distance of x cm from the surface of the snow layer, is given by

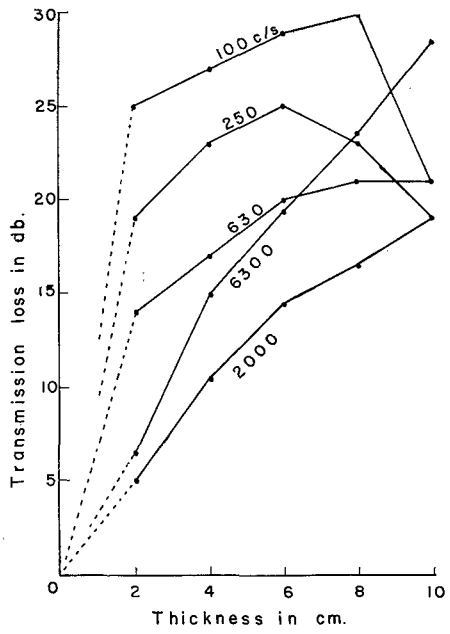

Fig. 27. Transmission loss *vs.* thickness of compact snow (density: 0.35 g/cm^3, flow resistance: 19.8 g/s·cm^3). Numbers indicate frequency of sound in c/s

$$p = p_0 e^{-\alpha x}, \tag{23}$$

where p_0 is the sound pressure at the surface of snow on the source side, and α is the attenuation constant in 1/cm. Moreover, if it is assumed that the sound levels L_1 and L_2 in Eq. (22) are expressed by p_0 and p as follows:

$$\left.\begin{aligned} L_1 &= 20 \log_{10} p_0 \\ L_2 &= 20 \log_{10} p , \end{aligned}\right\} \tag{24}$$

then, combining Eqs. (22), (23), and (24), we have

$$TL = 20 \log_{10} \frac{p_0}{p} = (20 \alpha \log_{10} e) x. \tag{25}$$

Equation (25) means that the transmission loss is linearly proportional to the thickness. This equation, however, may not be applied to explain the experimental results shown in Fig. 27. As shown in this figure, the TL *vs.* thickness curves measured at low frequencies exhibit maxima at certain thicknesses. It may be assumed that, when a low frequency sound wave penetrates a comparatively thick sample, a standing wave may be formed by resonance within the sample causing an apparent decrease in the transmission loss. The reason why the transmission loss does not dip at high frequencies in a thick sample, may be that the attenuation of sound is very high at high frequencies in thick samples and it is impossible to form a standing wave such samples. As is shown in Fig. 27, curves for TL *vs.* thickness are almost straight lines at thicknesses between 2 and 6 cm. Therefore, the attenuation, constant, α, in this snow may be

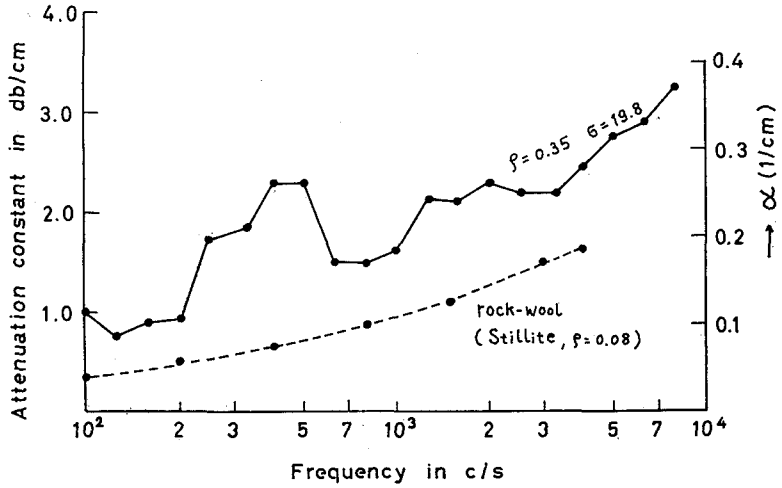

Fig. 28. Frequency characteristics of the attenuation constant of compact snow (density: 0.35 g/cm³, flow resistance: 19.8 g/s·cm³). The dotted curve shows the attenuation constant of Stillite (After SCOTT)

calculated from the gradient of each straight line. Figure 28 shows the ferquency dependence of the attenuation constant of compact snow (density: 0.35 g/cm³, flow resistance: 19.8 g/s cm³) obtained in this manner. In this figure, the frequency dependence of the attenuation constant of Stillite (bulk density: 0.080 g/cm³) obtained by SCOTT (1946) is shown by the broken curve. He measured the α of Stillite directly by inserting a small probe-tube microphone into it. It is difficult, however, to apply his method to the snow, since the texture of the snow may be destroyed by the insertion of a probe-tube microphone. As is shown in Fig. 28, the frequency dependence of the attenuation constant of compact snow has tendencies which are similar to that of the porous material, Stillite.

In order to show how the *TL* changes in various kinds of snow, *TL* curves for overall white noise were drawn for three samples of varying thickness (Fig. 29). As is

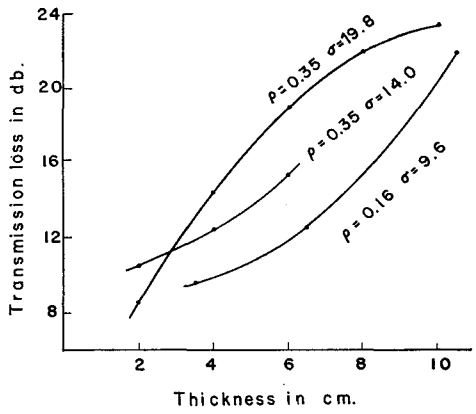

Fig. 29. Transmission loss *vs.* thickness of snow layer for overall white noise

shown in this figure, in the samples more than 4 cm thick, the smallest TL was obtained in new snow with a density of 0.16 g/cm^3 and a flow resistance of 9.6 g/s·cm^3, and the TL was larger in compact snow with a flow resistance of 19.8 g/s·cm^3 than in compact snow with a flow resistance of 14.0 g/s·cm^3, although the density of these samples was the same, 0.35 g/cm^3. This may be explained by the difference in their flow resistance, since transmission loss or attenuation of sound pressure in snow layers results primarily from viscous resistance of air in small snow pores. According to MORSE (1952), the relation between the attenuation constant and flow resistance in porous materials is given by

$$\alpha = A\sqrt{\omega \cdot \sigma}\,, \tag{26}$$

where α is the attenuation constant, ω the angular frequency, σ the flow resistance, and A is a constant independent of the frequency. Figure 30 shows the relation between the attenuation constant and flow resistance, obtained for overall white noise through various kinds of snow samples, all less than 5 cm

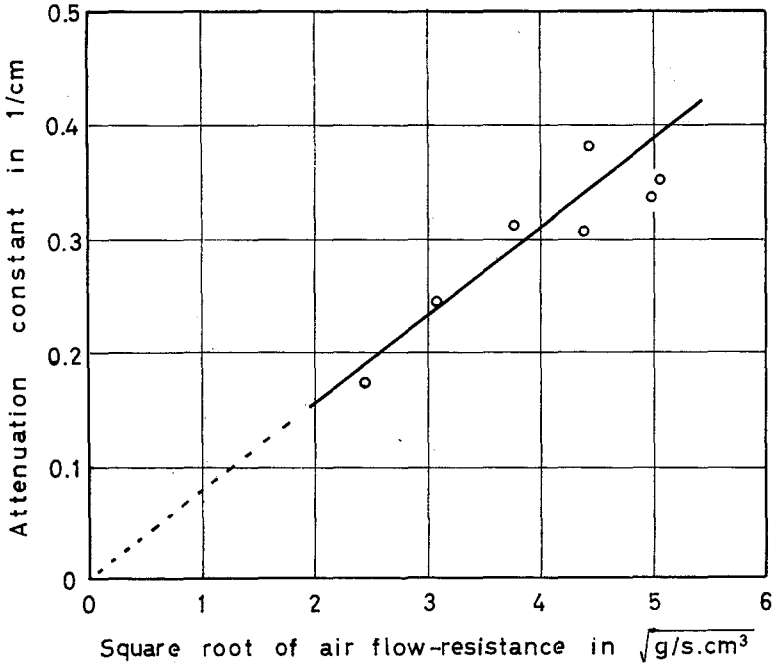

Fig. 30. Relation between attenuation constant and square root of flow resistance for overall white noise through various snow samples less than 5 cm thick

thick. It is interesting that MORSE's equation can be applied to consolidated materials such as snow.

VI. Attenution on Sonw Surfaces

The acoustic characteristics of small samples of natural snow covers have been investigated in the laboratory. In this section, the problems of sound propagation in open snow fields are treated. Experiments were made in Feb. 1958 on a snow field approximately 100×300 m at the forest experimental station of Hokkaido University in Moshiri, Hokkaido. The snow field was surrounded by few trees, and was quiet enough to conduct acoustical experiments. A density profile of the snow cover is shown in Fig. 31.

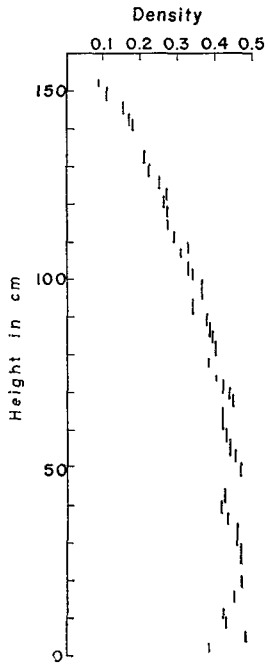

Fig. 31. Vertical density distribution in the snow cover, used for sound propagation experiments

A moving-coil loud-speaker mounted on an enclosed spherical cabinet was used as the source of white noise. The intensity of the sound was measured in every 20 frequency band between 100 and 8,000 c/s with a sound level meter and 1/3 octave band-pass filters.

Figure 32 shows the intensity distribution of the sound field on the surface of the snow cover at every frequency band. The relative location of the sound source and the sound level meter is shown in the lower right hand corner of this figure. The length of each side of a square block is 2 m. The numbers on the top of the tetragonal frames indicate the centre frequency of 1/3 octave bands. The number adjacent to each contour indicates the sound level, measured in db. The sound source had no directivity in the plane perpendicular to the axis of the loud-speaker, but had appreciable directivity in the plane of the axis. The loudspeaker was set at a height of 35 cm above the surface of snow cover so that its axis was parallel to the surface of snow cover. Since the directional patterns of the sound field were symmetrical on both sides of the axis of the loud-speaker, only the second quadrant of the pattern is shown in Fig. 32. As is shown in this figure, the directional patterns of the sound field appear to be concentric circles around the source in the low frequency range below 1,000 c/s, but the weak directional

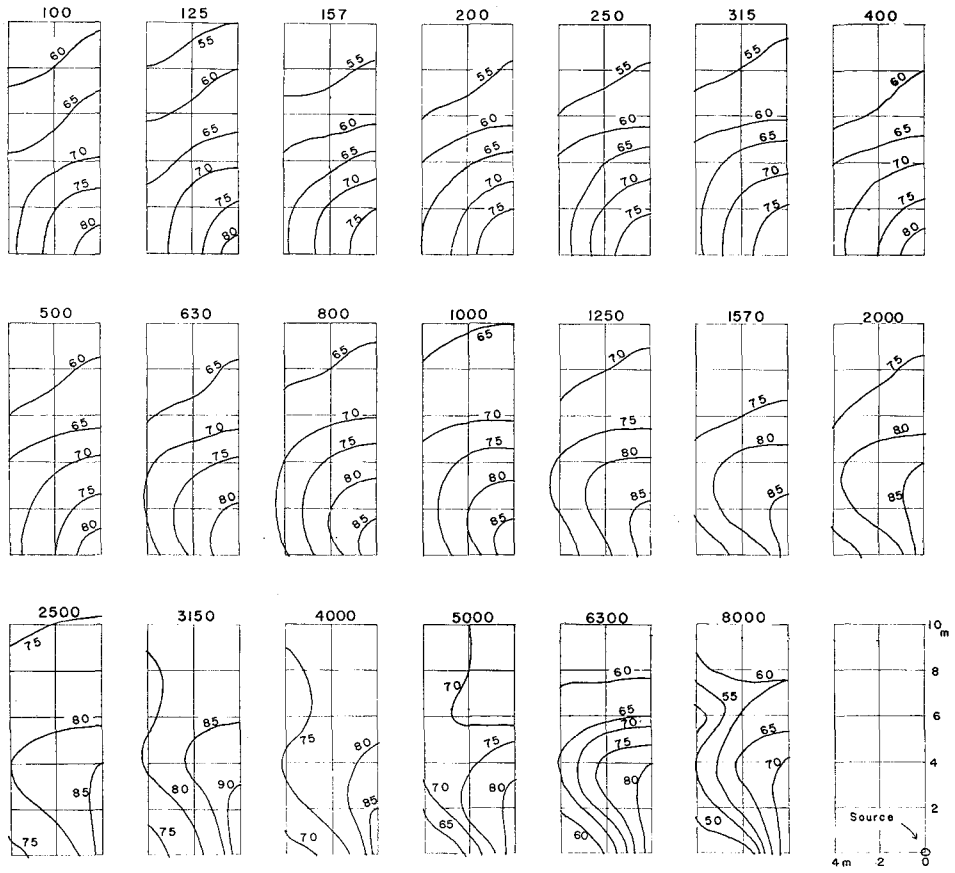

Fig. 32. Sound field on the surface of a snow cover. Numbers at the top of each square indicate the centre frequency of 1/3 octave bands, in c/s

characteristics of the pattern can be seen in the middle frequency range between 1,250 and 2,500 c/s, and the patterns are fairly confused in the high frequency range above 3,150 c/s. These variations in the sound field are more related to the characteristics of the sound source than to those of the snow cover surface. Therefore, further measurements of sound field were only made along the axis of the loud-speaker where the sound field was not confused.

The vertical distribution of sound intensity above the surface of the snow cover was measured at a distance of 6 m beyond the source. As is shown in Fig. 33, the intensity of the overall white noise decreased rapidly near the surface of snow cover. This implies that the sound field was intensly affected close to the surface of the snow cover. Figure 34 shows the intensity of

sound in the vicinity of the mouth of a HELMHOLTZ's resonator placed facing the sound source (SATŌ and KUBO 1938). When the resonator does not resonate with the source, the intensity of sound decreases rapidly with its approach to the mouth of the resonator, as is shown by curve (b). The vertical distribution of sound intensity shown in Fig. 33 is quite similar to curve (b) in Fig. 34. Therefore, the snow surface can be considered as a HELMHOLTZ's resonator with a different resonance than the source. In a previous section, the characteristics of the acoustic impedance of new snow were explained by an acoustic model composed of a narrow tube and a large cavity. This model may be regarded as a HELMHOLTZ's resonator.

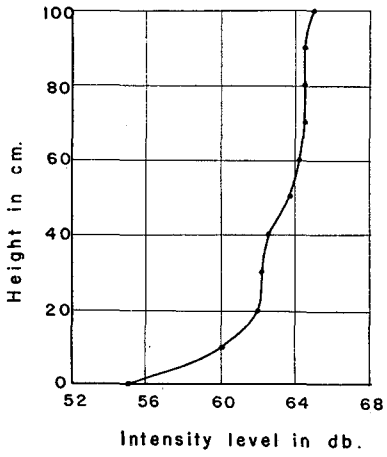

Fig. 33. Vertical distribution of sound intensity above the surface of a snow cover

As is shown in Fig. 33, a sound field higher than 30 cm is not disturbed by the surface of the snow cover. This may be proven by the following experiment: The attenuation of sound was measured along the axis of a loud-speaker mounted at a height of 35 cm above the surface of the snow cover. The attenuation curves obtained in this experiment in

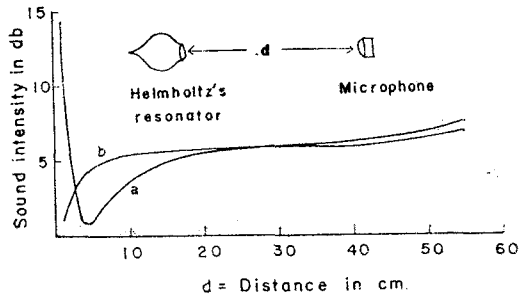

Fig. 34. Sound intensity near the mouth of a resonator placed facing the sound source
(a) resonator is resonant with the source at 250 c/s
(b) resonator is not resonant (After SATŌ et al.)

every frequency band may be expressed by "the law of inverse squares" as may be seen in Fig. 35, where each curve has been shifted along the ordinate so that the curves are not superimposed. This means that, at a height of 35 cm,

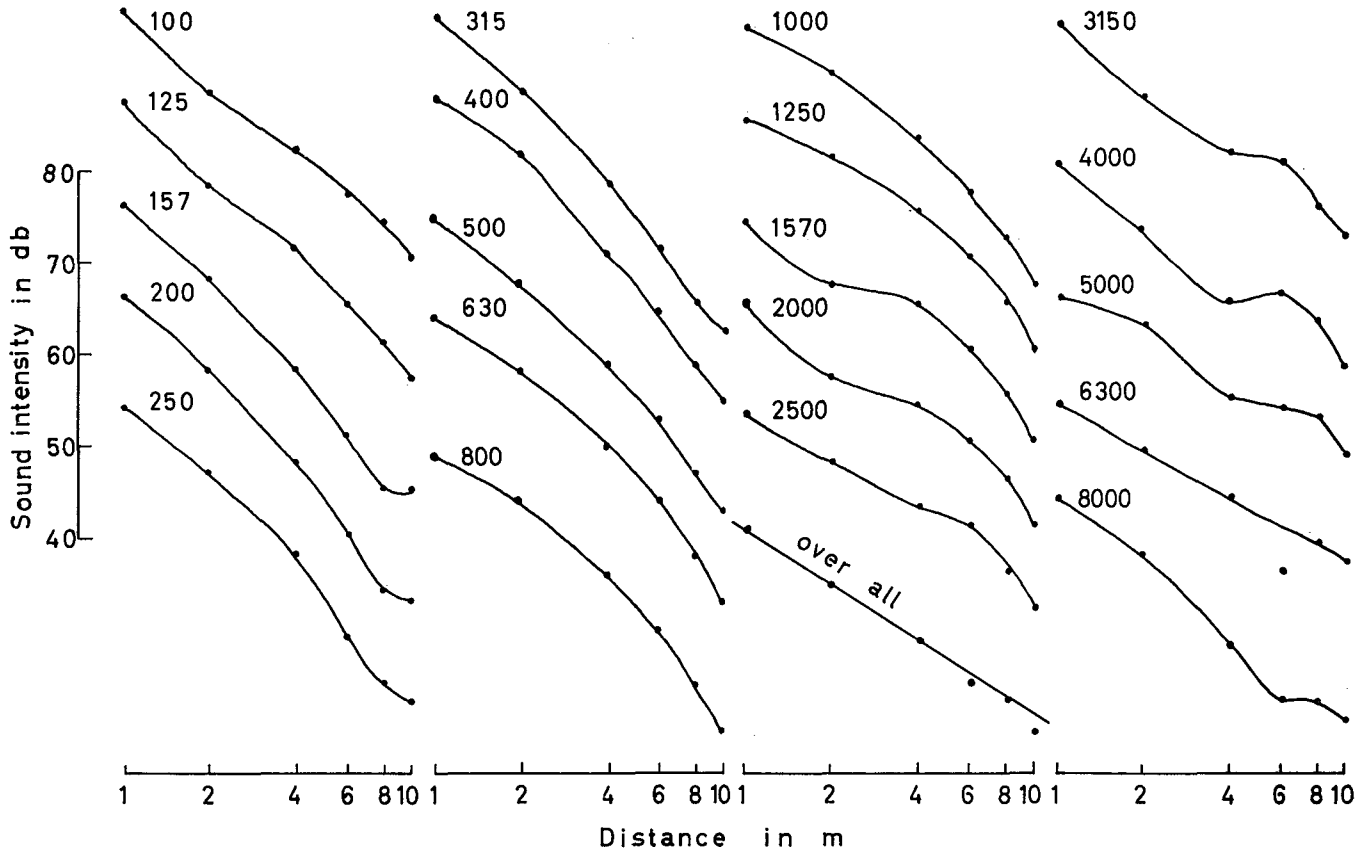

Fig. 35. Attenuation of sound measured along the axis of a loud-speaker at a height of 35 cm above the surface of a snow cover. Numbers indicate center frequency of 1/3 octave bands, in c/s

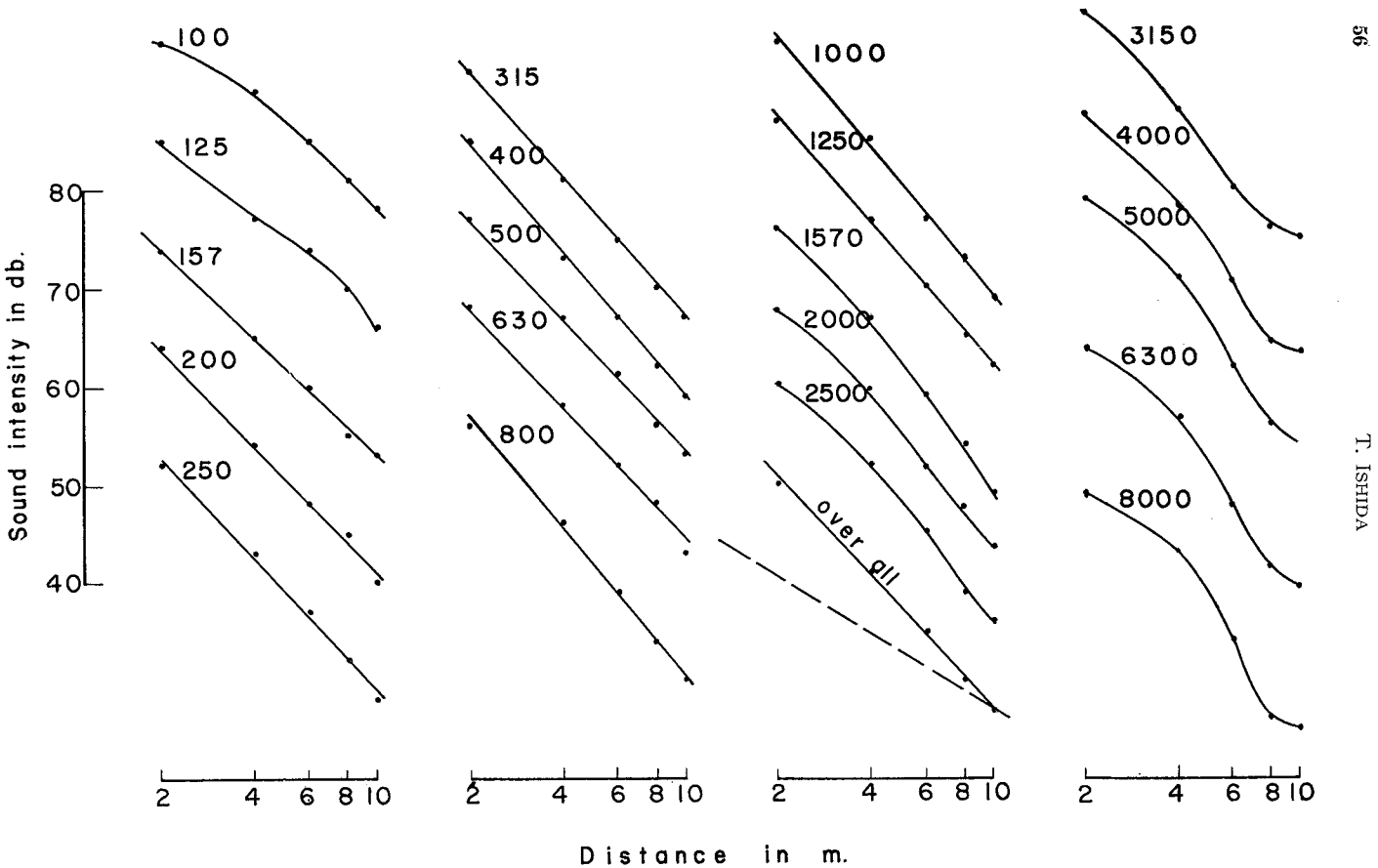

Fig. 36. Attenuation of sound measured at the surface of a snow cover and on a line parallel to the axis of a loud-speaker. Numbers indicate the center frequency of 1/3 octave bands in c/s. Broken lines indicate conformation with law of inverse squares

sound propagation is not disturbed by the surface of the snow cover and is similar to propagation in free space or in an anechoic chamber, where the decrease in the intensity of sound is inversely proportional to the square of the distance from the point source. On the other hand, there was great deviation from this "law of inverse squares" when the attenuation of sound was measured at the surface of snow cover on a line parallel to the axis of the loud-speaker. Steep attenuation curves were obtained in all frequency bands as is shown in Fig. 36.

Sound waves are propagated nearly spherically, from the source to the surface of the snow cover as may be seen in Fig. 32. Therefore, if the sound pressure on the surface of the snow cover at a distance of 1 m beyond the source is p_1, the sound pressure on the surface, p_x, at the any distance, x m beyond the source, is given by

$$P_x = p_1 x^{-1} e^{-\alpha x}, \tag{27}$$

where α is the attenuation constant on the surface of the snow cover. If the intensity levels measured for p_1 and p_x are given by

$$\left.\begin{aligned} L_1 &= 20 \log_{10} p_1, \\ \text{and} \quad L_x &= 20 \log_{10} p_x, \end{aligned}\right\} \tag{28}$$

the attenuation constant α is

$$\alpha = \frac{L_1 - L_x - 20 \log_{10} x}{20 \log_{10} e}. \tag{29}$$

The frequency characteristics of the attenuation constants calculated from the data given in Fig. 36 using Eq. (29), are shown in Fig. 37. At first sight, this appears similar to the attenuation characteristic curve in compact snow shown in Fig. 28, but the actual value of the attenuation constant on the surface of snow cover is about 1/100 of that in compact snow. For example, the distance at which the intensity of a sound of 1 kc is reduced to 1/100, is 12.5 cm in compact snow, and 13.5 m on the surface of a new snow cover.

In order to observe sound propagation in a snow trench and in a tunnel, a trench, $1 \times 11 \times 1.4$ m, was dug in snow cover, and a tunnel $80 \times 310 \times 80$ cm was bored at a depth of 45 cm from the surface of snow cover through the snow-wall at one end of the trench. Since the original depth of snow cover was 1.5 m, the bottom of the trench and the tunnel was 10 cm thick. A sketch of the trench and tunnel is shown in Fig. 38. A spherical loud-speaker was placed in the innermost part of the tunnel as a source of white noise. The walls of the trench and the tunnel were primarily composed of compact snow

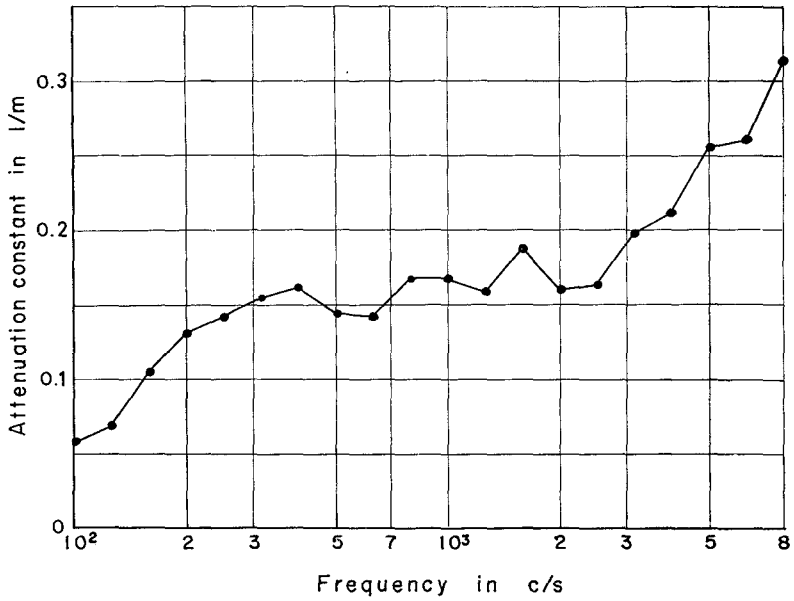

Fig. 37. Frequency characteristics of attenuation constant at the surface of a snow cover

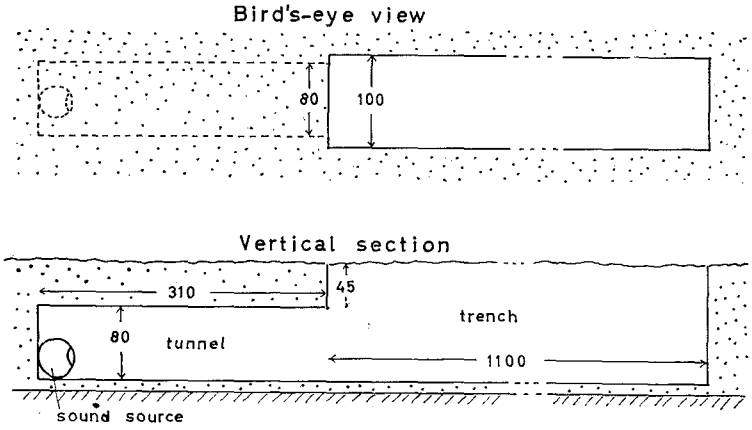

Fig. 38. Snow tunnel and trench (dimensions in cm).

with a density of 0.30—0.45 g/cm^3, but the snow on the bottom of the trench was packed hard by walking on it.

The sound intensity levels in the trench and the tunnel, measured along the axis of the loud-speaker, are shown in Fig. 39, where the measured values are plotted and shifted along the ordinate for every frequency so that the plotted

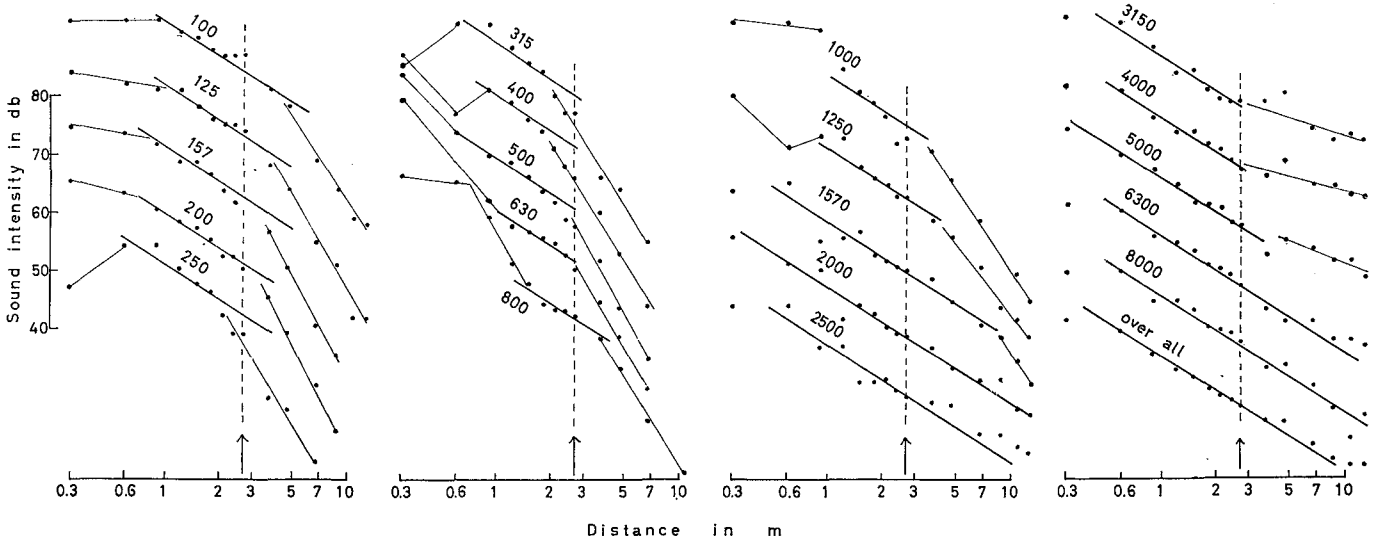

Fig. 39. Attenuation of sound in a snow tunnel and trench. Arrows show the location of the mouth of the tunnel. Tunnel extends to left of the arrows. Heavy lines indicate conformation with the law of inverse squares. Numbers indicate the centre frequency of 1/3 octave bands, in c/s

points are not superimposed. In this figure, the arrow indicates the location of the mouth of the tunnel, and the curves to the right of this arrow indicate the sound level distribution in the trench, and those to the left of the arrow the distribution in the tunnel. In these curves, thick solid lines indicate that the attenuation obeys the inverse square law. The attenuation curve for overall white noise is well expressed by the law of inverse squares, except in the vicinity of the sound source and at the end of the trench. This deviation or edge effect at both ends of the trench and tunnel may be caused by sound reverberation from the snow-wall beyond. According to these experiments, the absorption coefficients of compact snow (density: 0.33–0.37 g/cm^3, thickness: 10 cm) range from 0.8 to 0.6. Therefore, the walls of the trench and tunnel may reflect approximately 20–40% of incident sound energy. As may be seen in Fig. 39, the majority of the attenuation curves consist of three parts with different slopes against abscissa. In the first part, within 1 m of the source, the curves slope gently. In the second part from 1 m beyond the source to the mouth of the tunnel, the majority of the curves express the law of inverse squares. In the third part, inside the trench, there are fairly steep slopes.

The attenuation characteristic for frequency in the first part of the curves is not systematic, because of sound reverberation from the snow-wall beyond the sound source and because it is too close to the source. In the second part of the curves, the sound attenuates in accordance with the law of inverse squares, in all frequency bands. In this region, the conditions are the same as those in an anechoic chamber, because there is no reverberation from the inside snow-wall or the mouth of the snow-tunnel. In the third part, the attenuation curves show steep gradients from the mouth of tunnel, through the trench. This means that the mechanisms of attenuation are quite different in the tunnel and the trench. Since it can be assumed that the sound is apparently emitted from the mouth of the tunnel into the trench, the mouth of the tunnel may be regarded as an imaginary sound source, the dimension of which is 80×80 cm. When the sound source is not a point source, the true location of the source may be graphically determined as follows: Inverse values of sound pressure are plotted against the distance from the position of the source. A curve which connects these points is extrapolated until it intersects with the abscissa. The intersection gives the true location of the source where the sound pressure becomes infinite. In general, the locaiton of the source may differ as a function of the frequency.

Applying this procedure for sound radiation from the mouth of the tunnel, we determined the true location of the source at intervals approximately 1, 2,

and 2.7 m beyond the mouth of the tunnel for frequencies less than 630 c/s, between 800 and 1,570 c/s, and above 2,000 c/s, respectively. The last distance, 2.7 m, agrees with the original location of the loud-speaker. Using these values, we can calculate the attenuation levels based on the law of inverse squares, in which the sound source would exist at each of the locations stated above. If we subtract these attenuation levels from the observed attenuation levels shown in Fig. 39, we obtain the attenuation constant based upon the assumption that

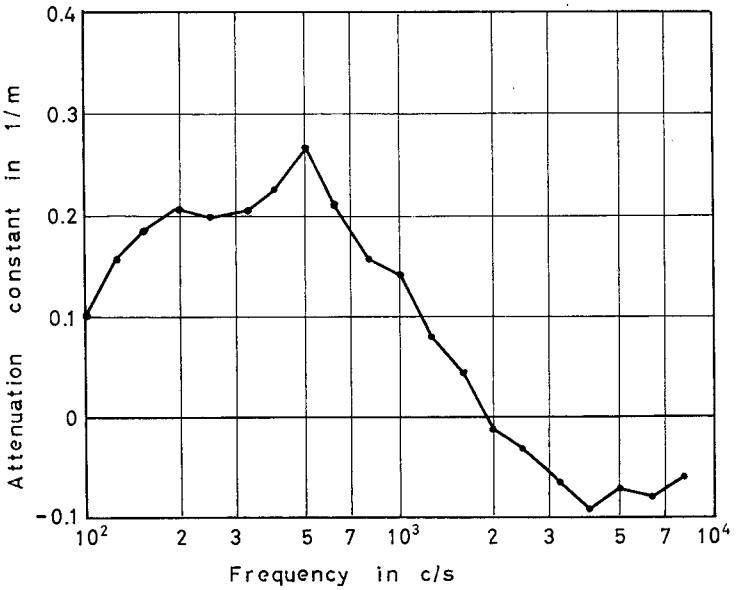

Fig. 40. Frequency characteristics of the attenuation constant in a snow trench

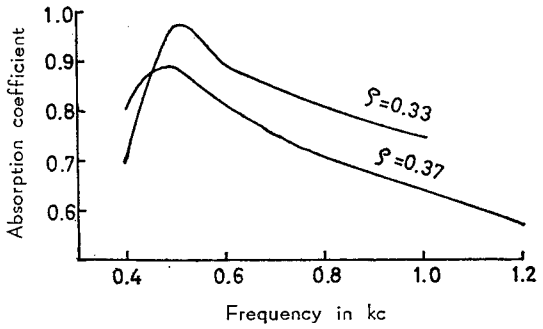

Fig. 41. Frequency characteristics of the absorption coefficient of compact snow (density: 0.33 and 0.37 g/cm^3)

plane waves of sound are propagated in the trench, as is shown in Fig. 40. The frequency characteristic of the attenuation constant is maximum around a frequency of 500 c/s. This is similar to the frequency characteristic of the absorption coefficient of compact snow shown in Fig. 41. The attenuation constants in the trench are negative in the high frequency range above 2 kc. This indicates that attenuation is apparently smaller at high frequencies than it is in free space because of the generation of reverberation by the slight absorption in the walls of compact snow.

VII. Concluding Remarks

The observed acoustic impedance characteristics for snow layers of various thicknesses are well explained, both by an acoustical model consisting of a narrow tube und a large cavity, and by an electrical model composed of a *C-R* recurrent network. The acoustic impedance of compact snow had smaller reactance and higher resistance than that of new snow. Although the change in the reactance of compact snow was insignificant, the resistance of the snow increased with density. Moreover, the resistance of the compact snow was very sensitive to its internal structure: grain size, shape, and ice-bonding, even when the density was the same.

The sound velocity in compact snow, as estimated from measured values for acoustic impedance, increased with the sound frequency used and with the porosity of the snow sample. This conclusion may be qualitatively explained by analogy with transmission lines consisting of continuously distributed impedance and admittance.

The attenuation constants of sound waves in snow layers were obtained by measuring transmission loss through the layers. It was found that the attenuation constants were proportional to the square root of the air flow resistance through the snow layers. Investigations of the propagation of white noise on the surface of a snow cover and in a snow trench, showed that the frequency-response curves of their attenuation constants were parallel to those of their absorption constants, and that the attenuation constant through a snow sample was 100 times larger than that on the surface.

The acoustic properties of snow obtained by these investigations may be useful, not only in understanding the compex structure of snow, but also in providing information for acoustical projects in snowy regions.

Acknowledgement

The author wishes to express his gratitude to Dr. H. ŌURA and Dr. D. KUROIWA for encouragement and valuable advice in the preparation of this manuscript. He also is indebted to Mr. H. SHIMIZU for his assistance in measuring the flow resistance of snow.

References

ANDŌ, I. and HOSOKAI, M. 1952 Attenuation of acoustical properties of the snow. Studies in Fallen Snow, Scientific Institute for Research in Fallen Snow, Nagaoka, No. 4, 67–74. (In Japanese).

BERANEK, L. L. 1940 Precision measurement of acoustic impedance. J. Acous. Soc. Am., **12**, 3–13.

FURUKAWA, I. 1953 A study on the absorption of sound by snow. Yuki-to-seikatsu, The Snow Association of Japan, Niigata, **5**, 30–32. (In Japanese).

ISHIDA, T. and ONODERA, S. 1954 Sound absorption by snow layer.* Low Temperature Science, A **12**, 17–24.

ISHIDA, T. and SHIMIZU, H. 1956 Determination of the resistance to air flow of snow layer. II. Portable σ-meter.* Low Temperature Science, A **15**, 63–71.

KINOSITA, S. and WAKAHAMA, G. 1959 Thin sections of deposited snow made by the use of aniline.* Low Temperature Science, A **18**, 77–96.

MOSE, R. W. 1952 Acoustic propagation in granular media. J. Acous. Soc. Am., **24**, 696–700.

ŌURA, H. 1953 a Sound velocity in snow cover.* Low Temperature Science, **9**, 171–178.

ŌURA, H. 1953 b Reflection of Sound at snow surface and mechanism of sound propagation in snow.* Low Temperature Science, **9**, 179–186.

SATŌ, K. and KUBO, K. 1938 On the influence of a resonator upon the sound field.* Rep. Aero. Res. Inst., Tokyo Univ., **8**, 237–244.

SCOTT, R. A. 1946 a An apparatus for accurate measurement of the acoustic impedance of sound-absorbing materials. Proc. Phys. Soc., **58**, 253–264.

SCOTT, R. A. 1946 b The absorption of sound in a homogeneous porous medium. Proc. Phys. Soc., **58**, 165–183.

TAKADA, M., OHKHOCHI, S., and NASU, N. 1954 On the absorption coefficient of snow and the propagation of sound along snow surface.* J. Acoust. Soc. Japan, **10**, 23–27.

WENTS, E. C. and BEDELL, E. H. 1928 Measurement of acoustic impedance and the absorption coefficient of porous materials. Bell System Technical Jour., **7**, 1–10.

ZWIKKER, C. and KOSTEN, C. W. 1949 Sound absorbing materials. Elsevier, New York, P. 23 *et seq.*

* In Japanese with English résumé.